

GRAPHITE, TUBULAR PAHs, AND THE DIFFUSE INTERSTELLAR BANDS

ZHIYONG ZHOU,¹ MATTHEW Y. SFEIR,¹ LEI ZHANG,¹ MARK S. HYBERTSEN,² MICHAEL STEIGERWALD,¹ AND LOUIS BRUS¹

Received 2005 October 12; accepted 2006 January 6; published 2006 January 26

ABSTRACT

Planar polycyclic aromatic hydrocarbons (PAHs) are candidates for the diffuse interstellar band (DIB) carriers. Nanometer-size Fe metallic particles, expected to be present during astrophysical graphite growth, are catalytic for formation of a related species—large tubular PAH molecules. We propose that tubular PAH molecules are a component of the interstellar medium. Electronic structure calculations, on a specific family of tubular PAH molecules derived from elongated C₆₀, reveal intense electronic transitions in the visible and near-IR, which vary systematically with length. We analyze these molecules as DIB carriers within the known constraints.

Subject headings: astrochemistry — dust, extinction — ISM: molecules — stars: carbon

1. INTRODUCTION

Interstellar dust clouds exhibit several hundred absorption features in the visible and near-IR spectral regions, known as the diffuse interstellar bands (DIBs; Fulara & Krelowski 2000; Snow 2001; Tielens & Snow 1995). The stronger DIBs were first observed in the 1920s. Modern high-sensitivity spectra show many weaker DIBs; there seems to be a transition every few angstroms across the visible and near-IR spectrum (Galazutdinov et al. 2005; Cox et al. 2005). It is thought that essentially every DIB has a different molecular carrier. These ubiquitous features have resisted identification despite systematic effort.

Carbon-containing species are a major component of the interstellar medium (ISM; Henning & Salama 1998). Planar polycyclic aromatic hydrocarbons (PAHs) in dust clouds are thought to emit vibrational IR luminescence (Sellgren 2001); such PAHs account for about 15% of the dust carbon (Allende Prieto et al. 2002). Specific PAH structures responsible for the IR luminescence have not been identified. Larger compact graphitic particles are thought to be responsible for 2175 Å bump in the dust ultraviolet scattering and extinction; perhaps 25% of the carbon is in some sort of graphitic particles (Draine 2004). Specific structures for fullerene-like concentric shell graphite particles (“bucky onions”) have been proposed for the 2175 Å bump carrier (Henrard et al. 1997; Tomita et al. 2004; Iglesias-Groth 2004). Note that quoted percentages are approximate as the C, O, Si, and Fe abundances in the ISM are still under debate (Li 2005).

Both large planar PAHs (neutrals and cations) and odd-numbered C₁₅–C₃₁ linear bare C chains are being investigated as possibly being part of the DIB carrier family (for a review, see Schmidt & Sharp 2005). More generally, the broad fullerene family and specifically C₆₀⁺ have been discussed in this context (Kroto & Jura 1992; Foing & Ehrenfreund 1997). All shorter C_n chains, smaller PAHs, and smaller fullerenes, whose spectra have been measured in laboratory experiments, do not reproduce the DIB spectra. In this Letter we describe how a closely related species—tubular PAHs, based on the metallic single wall carbon nanotube of the same diameter as C₆₀—are calculated to have the systematic, intense visible and near-IR op-

tical transitions expected of the DIB carrier family. Moreover, there is a clear experimental pathway to their formation: recent laboratory experiments show that such short carbon nanotubes are catalytically formed at and above 1000 K on nanometer-size-reduced Fe particles, of the type expected in the circumstellar atmospheres of C-rich stars.

2. ASTROPHYSICAL GRAPHITE NUCLEATION AND PAH FORMATION

Graphitic particles are thought to form in the cooling outflow of asymptotic giant branch carbon-rich and Wolf-Rayet stars, in the ejecta of supernovae explosions, and possibly in shocked ISM dust clouds. In the hydrogen-dominated outflow of C-rich stars, equilibrium thermodynamics predicts that bulk graphite forms (from C₂H₂ principally) as the temperature cools through 1700 K (Sharp & Wasserburg 1995). A central issue is the rate and type of graphite (and PAH) nucleation. In nucleation theory there is a critical nucleus size; smaller clusters are not stable with respect to sublimation back into the vapor phase. The critical size is proportional to the surface energy, which is especially large in graphite with its huge covalent bond energy. With this large nucleation barrier, a model calculation predicts that the hot vapor will supercool to about 1200 K if the C/O ratio is near 1.2 (Chigai et al. 1999). In other work, a general chemical kinetic framework for graphite formation has been outlined for C-rich stars (Pascoli & Polleux 2000). Near Wolf-Rayet stars, hydrogen is absent; kinetic simulations show C₂ as the dominant reagent for graphite formation. There is no clear route to graphite formation using the known reactions in Wolf-Rayet outflows (Cherchneff et al. 2000). In supernova outflows and shocks, a possible nucleation process has been numerically modeled (Clayton et al. 2001). In all of the cases above nucleation remains speculative, in view of the many unknown reaction rates and uncertain astrophysical data.

As the temperature cools and entropy decreases, some reactions remain in equilibrium and shift toward products. Other reactions with high activation energy may go out of equilibrium. In the atmosphere of C-rich stars, the 3H₂ + CO → CH₄ + H₂O reaction at equilibrium should make gaseous H₂O at low concentration. Yet it was a surprise when OH from H₂O photodissociation was experimentally observed (Melnick et al. 2001), as it is hard to imagine a feasible gas-phase collisional reaction pathway. The reaction might actually occur by Fischer-Tropsch catalysis on the surface of nanometer metallic Fe particles (Latter & Charnley 1996). Order-of-magnitude kinetic calculations show the feasibility of this surface process (Willacy

¹ Department of Chemistry, Columbia University, 3000 Broadway, New York, NY 10027.

² Department of Applied Physics and Applied Mathematics and Center for Electron Transport in Molecular Nanostructures, Columbia University, 500 West 120th Street, New York, NY 10027.

2004). Such reduced, metallic Fe particles are predicted to form near 1300 K (ignoring supercooling) as the typical C-rich star atmosphere cools (Jones 1990; Sharp & Wasserburg 1995).

The average solar abundance of iron is about 10% of that of carbon. Laboratory work in the past decade has shown that transition metals (at a few mole percent relative concentration to carbon) have a pronounced catalytic effect on high-temperature graphite nucleation and growth, from carbon-rich vapor (Bethune 2002). On the surface of 1–10 nm Fe particles at temperatures of 1000 K and above, hydrocarbon reagents at low pressure make nanotube graphite almost exclusively (for a review, see Moisala et al. 2003). Carbon atoms from dissociative chemisorption are mobile on the hot particle; as the carbon “solubility limit” is reached, a nanotube (of roughly the same diameter as the particle) grows out of one side (Ding et al. 2004). This is the whisker growth mechanism long known in materials science (Wagner & Ellis 1964). A 1 nm diameter single wall carbon nanotube (SWNT) can grow to lengths of hundreds of microns if gaseous reagents are continuously supplied (Hafner et al. 1998; Kong et al. 1998). CH_4 , C_2H_2 , methyl alcohol, benzene, and toluene at low concentration in H_2 carrier gas have all been used as reagents. A few percent added H_2O has no effect on tube growth. With a pure high-pressure CO reagent, tubes grow as CO disproportionates to graphite and CO_2 (Nikolaev et al. 1999). In laser ablation or arc discharge experiments on graphitic targets with a few percent added transition metal, nanotubes grow from gaseous elemental carbon reagents in the cooling plasmas (Thess et al. 1996). In these experiments the catalytic effect of Fe nanoparticles is well established.

Fe nanoparticles are catalysts when equilibrium thermodynamics predicts tubular graphite formation at the specific temperature and partial pressures considered, as shown in a recent careful experiment with CH_4 (Wagg et al. 2005). As described above, growth experimentally occurs in the presence of surface O or H atoms, or other simultaneous reactions such as the Fischer-Tropsch process. Fe particles also catalytically convert amorphous graphite into tubular graphite (Ichihashi et al. 2004). It would seem that any C-rich feedstock, including planar PAH species and/or nanometer amorphous graphite grains, could be converted to tubular graphite on Fe particles, if the overall reaction is thermodynamically allowed. In a cooling star outflow, if it happens that PAH or other graphitic molecules begin to form before nanometer Fe particles appear, these materials could be subsequently catalytically processed into tubular PAHs. Conversely, in supernovae there is meteorite evidence that iron does condense before graphite (Croat et al. 2003). Thus, catalytic formation of tubular graphite may be general.

In laboratory experiments the Fe catalytic particle is observed attached to the SWNT at one end. Several concentric shells of graphitic carbon are observed around the nanometer Fe particles in TEM images—the iron carbide FeC catalytic nanoparticle thought to be present at high temperature during growth undergoes phase separation into Fe with concentric carbon, as the particle cools (Bladh et al. 2000).

Equilibrium thermodynamic simulations also predict that solid SiC and TiC grains will form, along with reduced Fe particles, as C-rich star atmospheres cool. Unlike the FeC analogs, SiC and TiC do not phase-separate at low temperature. Features in the interstellar IR spectra of C-rich star atmospheres have been assigned to SiC and TiC grains (Henning & Mutschke 2001). In laboratory experiments, Si and Ti are not catalytic for formation of nanotube graphite, in contrast to Fe. But such carbide particles could serve as nuclei for growth of concentric

graphite; this process has been numerically simulated for C-rich stars (Chigai et al. 1999; Bernatowicz et al. 2005). Meteorites contain presolar dust grains with distinctive isotopic signatures. In the Murchison meteorite, about one-third of the many spheroidal onion graphite grains examined had nanometer-size metallic (Ti, Mo, Zr) carbide inclusions (Bernatowicz et al. 1996; Croat et al. 2005). These onion grains are larger than, yet analogous to, Fe catalytic particles recovered after SWNT laboratory synthesis. Stable, essentially entirely carbon $\text{C}_{100}\text{--C}_{400}$ molecular species (of unknown structure) have been found in the Allende meteorite by solvent extraction (Becker et al. 1999). TEM examination shows curved graphitic fragments and apparently closed single wall and multiwall round fullerene-like images (Harris et al. 2000). We expect that Fe/graphite core/shell particles hypothetically present in the meteorites should be not extracted by organic solvents.

3. TUBULAR PAH MOLECULES

If conditions exist to form concentric graphite shells around TiC and MoC grains in a hot, carbon-rich astrophysical environment, then nanotube graphite growth should be catalyzed by the nanometer-reduced Fe particles also present. Nanotube length would depend on the local Fe/C ratio, detailed chemical kinetics, and will vary with situation. Longer nanotubes would be broken into shorter lengths, and the Fe catalytic particles detached, by subsequent shock processing in the ISM. We propose that part of the graphite/PAH ISM dust material is short nanotube PAH stubs, with a wide distribution of different lengths and diameters, mostly with H-terminated ends. Such short tubular PAH molecules (as well as planar PAHs) would have optical absorption cross sections much larger than Rayleigh scattering cross sections; we would not expect them to contribute to the 2175 Å scattering bump.

Discovered just 12 years ago (Iijima & Ichihashi 1993), infinite SWNTs are seamless graphite tubes, without dangling bonds or pentagonal rings (for a review, see Saito et al. 1998). About 100 structurally different SWNTs are topologically possible for diameters less than about 2 nm. On a statistical basis, one-third of the tubes are metallic, and two-thirds are semiconducting. Electrical conductivity and optical transitions involve the π electrons. Each different infinite tube is a unique, ordered, molecular species having its own characteristic optical absorption and scattering spectra. Experimental optical studies of micron length SWNTs have appeared recently (Bachilo et al. 2002; Wang et al. 2005). The optical spectrum will also be a function of length and will only asymptotically approach the “bulk” infinite spectrum at lengths beyond several tens of unit cells. Laboratory studies of short tubular PAHs have not yet been reported.

Figure 1 shows the molecular structure of tubular $\text{C}_{160}\text{H}_{20}$, a hydrogen-terminated piece of the metallic (5, 5) SWNT. This specific SWNT is the infinite tubular limit of the C_{60} , C_{70} , C_{80} family. Note that C_{60}^+ itself is a possible carrier of the 9577 and 9632 Å DIBs (Foing & Ehrenfreund 1997). These tubular PAH molecules have HOMO (highest occupied molecular orbital) to LUMO (lowest unoccupied molecular orbital) gaps that decrease toward zero as the tube lengthens. In 2004 we performed electronic structure calculations on finite (5, 5) PAH molecules up to $\text{C}_{210}\text{H}_{20}$ using density functional techniques (Zhou et al. 2004); we now extend these calculations to $\text{C}_{490}\text{H}_{20}$. These species are stable, covalently bonded singlet molecules. Short stubs such as $\text{C}_{40}\text{H}_{20}$ have several optical transitions above 4.0 eV. As the tube lengthens beyond $\text{C}_{60}\text{H}_{20}$, one optical tran-

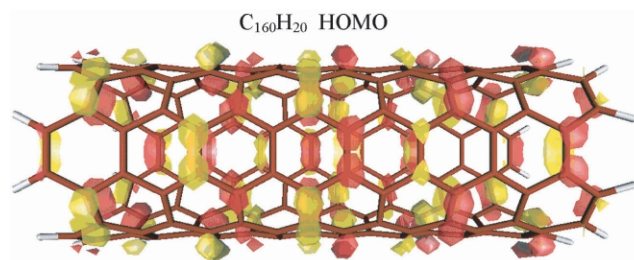


FIG. 1.—Geometrically optimized structure of $C_{160}H_{20}$ tubular PAH, composed of 8 unit cells of the (5, 5) infinite SWNT. The π electron HOMO orbital is shown.

sition (polarized along the axis) decreases in energy and increases in intensity, as shown in Table 1. In this tubular PAH family, the optical transition energies move through the visible and near-IR range of the DIBs. In the longest calculated species $C_{490}H_{20}$, the transition occurs at 0.61 eV with an oscillator strength of 12.4. A simple one-dimensional classical free-electron metal model predicts that finite PAHs derived from all metallic SWNT structures will have similar intense “charge transfer” optical transitions. In preliminary numerical calculations, PAHs based on larger diameter metallic (6, 6) tubes show that transitions of similar intensities and energies as in (5, 5) tubes are present.

This intense transition is an intrinsic property of π molecular orbitals delocalized along the tube length, as shown for the $C_{160}H_{20}$ HOMO shown in Figure 1. An earlier calculation on a short tube with C_{60} -type half-spherical end caps, instead of an H atom termination, also showed this intense transition (Jiang et al. 1997). This charge transfer absorption does not derive from the HOMO-LUMO transition. Two transitions contribute: the promotion of an electron from the HOMO to the first orbital above the LUMO and the promotion of an electron from the first orbital below the HOMO to the LUMO. In Table 1 the oscillator strengths for the two contributing orbital promotions have been added, and the two promotion energies averaged. At present, such calculated energies are not sufficiently accurate to predict exact DIB wavelengths. For the longer neutral species,

oscillator strengths from time-dependent density functional theory (TDDFT) calculations agree well with these values; the predicted TDDFT transition energies are about 0.3 eV higher (Zhou et al. 2004). TDDFT calculations are known to correctly reproduce the optical spectra of large planar PAHs, often with accuracies of about 0.2 eV (Halasinski et al. 2003).

4. CATIONS AND DIB CONSTRAINTS

A C_{12} – C_{13} isotopic shift model for DIB broadening, especially in the 6196 Å band, suggests that the carriers contain 50–100 C atoms (Walker et al. 2000; Webster 2004). This heterogeneous broadening must be present in any large carbon molecule system, independent of possible intrinsic internal broadening or Doppler broadening. The model rotational contours suggest that the species must be larger than C_{60} . Tubular PAHs seem consistent with these expected properties.

A photoionization model based on spectra taken in regions of different far-UV flux suggests that the 5797 and 6613 Å band carriers are cations (Sonnentrucker et al. 1997). We now calculate cation optical properties for sizes from $C_{80}H_{20}$ to $C_{190}H_{20}$. We use density functional theory (DFT) with the hybrid B3LYP functional and an atom centered basis; our method and calibration have been previously described (Zhou et al. 2004). Tubular PAH ions could form under astrophysical conditions: the adiabatic $C_{160}H_{20}$ ionization potential is 4.82 eV, and the electron affinity is 2.35 eV. A small molecular cation typically has a substantially different geometry and electronic structure than the neutral; thus, the cation optical spectrum is often completely different than that of the neutral. In contrast, we find that these large cations have optimized geometries and Kohn-Sham frontier orbitals essentially identical to those of the neutrals. The $C_{160}H_{20}$ Franck-Condon reorganization energy between neutral and cation is only 0.08 eV. The static DFT charge transfer orbital energy differences and dipole transition matrix elements are the same within 1%–2%. Thus, the cation will have the same intense visible and near-IR transition, with a shift of 0.1 eV or less, from the neutral. The cation oscillator strength shown in Table 1 is 25% lower because of the one missing HOMO electron.

The decrease in energy and increase in oscillator strength

TABLE 1
CALCULATED STATIC DFT CHARGE TRANSFER OPTICAL PROMOTION ENERGIES AND OSCILLATOR STRENGTHS FROM DIPOLE TRANSITION MATRIX ELEMENTS OF CONTRIBUTING TRANSITIONS, FOR TUBULAR PAH NEUTRALS AND CATIONS

NO. OF CARBON ATOMS	NEUTRAL		CATION	
	Transition Energy (eV)	Oscillator Strength	Transition Energy (eV)	Oscillator Strength
80	2.18	1.50	2.19	1.15
90	2.41	2.09	2.40	1.58
100	2.07	2.17	2.07	1.65
110	1.81	2.25	1.82	1.70
120	1.95	2.83	1.93	2.14
130	1.70	3.06	1.70	2.28
140	1.55	2.99	1.55	2.27
150	1.64	3.58	1.65	2.68
160	1.45	3.94	1.46	2.86
170	1.36	3.80	1.37	2.85
180	1.25	3.89	1.26	2.90
190	1.29	4.72	1.31	3.51
200	1.19	4.63
210	1.14	4.59
310	0.81	7.40
400	0.69	9.80
490	0.60	12.40

with length are similar to those predicted for the family of linear bare chains C_{15} – C_{31} that also approach metallic behavior at long length. In the carbon chain case, these calculated optical properties have made carbon chains a candidate for DIB carrier (Maier 2004, Maier et al. 2004).

Note, also, that tubular PAHs should have the size and rigidity thought to be necessary for survival against photodissociation in the interstellar medium (Allain et al. 1996). In addition, the tubular PAH species in Table 1 are highly symmetric (D5d or D5h point symmetry groups) and do not have a permanent dipole moment. Their microwave rotational transitions would be forbidden. Other possible tubular PAHs with less symmetric end passivation might be microwave-active.

5. CONCLUSION

Recent laboratory research has shown the pronounced catalytic effect of Fe nanoparticles on the high-temperature, gas-

phase nucleation of graphite. Thus, since Fe and carbon are relatively abundant in the ISM, short tubular PAHs should be present in the ISM. There should also be nanometer-size Fe particles with a few concentric graphite shells. Our calculations show that specific tubular PAHs (neutrals and cations) having the same diameter as C_{60} exhibit intense visible and near-IR transitions, consistent with expected DIB properties. Both experimental and further theoretical studies are needed to explore vibrational and other electronic properties of tubular PAHs.

This work was supported by DOE Basic Energy Sciences DFFG02-98ER 14861, by the NSF Nanoscale Science and Engineering Initiative CHE-0117752, and by the New York State Office of Science, Technology, and Academic Research (NYSTAR). Computational facilities are in part supported by the Columbia MRSEC DMR-0213574. L. B. thanks B. McCall, A. Witt, and R. Friesner for their stimulating discussions and correspondence.

REFERENCES

- Allain, T., Leach, S., & Sedlmayr, E. 1996, *A&A*, 305, 602
 Allende Prieto, C., Lambert, D. L., & Asplund, M. 2002, *ApJ*, 573, L137
 Bachilo, S. M., Strano, M. S., Kittrell, C., Hauge, R. H., Smalley, R. E., & Weisman, R. B. 2002, *Science*, 298, 2361
 Becker, L., Bunch, T., & Allamandola, L. 1999, *Nature*, 400, 227
 Bernatowicz, T., Akande, O., Croat, T., & Cowski, R. 2005, *ApJ*, 631, 988
 Bernatowicz, T., Cowsik, R., Gibbons, P., Lodders, K., Fegley, B., Amari, S., & Lewis, R. 1996, *ApJ*, 472, 760
 Bethune, D. 2002, *Physica B*, 323, 90
 Bladh, K., Falk, L. K. L., & Rohmund, F. 2000, *Appl. Phys. A*, 70, 317
 Cherchneff, I., Le Tueuff, Y. H., Williams, P. M., & Tielens, A. G. G. M. 2000, *A&A*, 357, 572
 Chigai, T., Yamamoto, T., & Kozasa, T. 1999, *ApJ*, 510, 999
 Clayton, D., Deneault, E., & Meyer, B. 2001, *ApJ*, 562, 480
 Cox, N., Kaper, L., Fonig, B., & Ehrenfest, P. 2005, *A&A*, 438, 187
 Croat, T. K., Bernatowicz, T., Amari, S., Messenger, S., & Stadermann, F. J. 2003, *Geochim. Cosmochim. Acta*, 67, 4705
 Croat, T. K., Stadermann, F. J., & Bernatowicz, T. J. 2005, *ApJ*, 631, 976
 Ding, F., Bolton, K., & Rosen, A. 2004, *J. Phys. Chem. B*, 108, 17369
 Draine, B. T. 2004, in *Origin and Evolution of the Elements*, ed. A. McWilliam & M. Rauch (Cambridge: Cambridge Univ. Press), 317
 Foing, B., & Ehrenfreund, P. 1997, *A&A*, 317, L59
 Fulara, J., & Krelowski, J. 2000, *NewA Rev.*, 44, 581
 Galazutdinov, G., Han, I., & Krelowski, J. 2005, *ApJ*, 629, 299
 Hafner, J., Bronikowski, M., Azamian, B., Nikolaev, P., Rinzler, A., Colbert, D., Smith, K., & Smalley, R. 1998, *Chem. Phys. Lett.*, 296, 195
 Halasinski, T., Weisman, J., Ruitkamp, R., Lee, T., Salama, F., & Head-Gordon, M. 2003, *J. Phys. Chem. A*, 107, 3660
 Harris, P., Vis, R., & Heymann, D. 2000, *Earth Planet. Sci. Lett.*, 183, 355
 Henning, Th., & Mitschke, H. 2001, *Spectrochim. Acta A*, 57, 815
 Henning, Th., & Salama, F. 1998, *Science*, 282, 2204
 Henrard, L., Lambin, P., & Lucas, A. 1997, *ApJ*, 487, 719
 Ichihashi, T., Fujita, J., Ishida, M., & Ochiai, Y. 2004, *Phys. Rev. Lett.*, 92, 215702
 Iglesias-Groth, S. 2004, *ApJ*, 608, L37
 Iijima, S., & Ichihashi, T. 1993, *Nature*, 363, 603
 Jiang, J., Xie, R.-H., Ma, J., & Yan, F. 1997, *Phys. Lett. A*, 231, 259
 Jones, A. 1990, *MNRAS*, 245, 331
 Kong, J., Cassel, A., & Dai, H. 1998 *Chem. Phys. Lett.*, 292, 567
 Kroto, H., & Jura, M. 1992, *A&A*, 263, 275
 Latter, W., & Charnley, S. 1996, *ApJ*, 463, L37 (erratum 465, L81)
 Li, A. 2005, *ApJ*, 622, 965
 Maier, J. P. 2004, in *The Dense Interstellar Medium in Galaxies*, ed. S. Pflanzner et al. (Heidelberg: Springer), 55
 Maier, J. P., Walker, G. A. H., & Bohlener, D. A. 2004, *ApJ*, 602, 286
 Melnick, G., Neufeld, D., Ford, K., Hollenbach, D., & Ashby, M. 2001, *Nature*, 412, 160
 Moisala, A., Nasibulin, A., & Kauppinen, E. 2003, *J. Phys. Condensed Matter*, 15, S30111
 Nikolaev, P., Bronkowski, M., Bradley, R., Rohmund, F., Colbert, D., Smith, K., & Smalley, R. 1999, *Chem. Phys. Lett.*, 313, 99
 Pascoli, G., & Polleux, A. 2000, *A&A*, 359, 799
 Saito, R., Dresselhaus, G., & Dresselhaus, M. S. 1998, *Physical Properties of Carbon Nanotubes* (London: Imperial College Press)
 Schmidt, T., & Sharp, R. 2005, *Australian J. Chem.*, 58, 69
 Sellgren, K. 2001, *Spectrochim. Acta A*, 57, 627
 Sharp, C., & Wasserburg, G. 1995, *Geochim. Cosmochim. Acta*, 59, 1633
 Snow, T. 2001, *Spectrochim. Acta A*, 57, 615
 Sonnentrucker, P., Cami, J., Ehrenfreund, P., & Foing, B. 1997, *A&A*, 327, 1215
 Tielens, A. G. G. M., & Snow, T. P., eds. 1995, *The Diffuse Interstellar Bands* (Dordrecht: Kluwer)
 Thess, A., et al. 1996, *Science*, 273, 483
 Tomita, S., Fujii, M., & Hayashi, S. 2004, *ApJ*, 609, 220
 Wagg, L., Hornyak, G., Grigorian, L., Dillon, A., Jones, K., Blackburn, J., Parilla, P., & Heben, M. 2005, *J. Phys. Chem. B*, 109, 10435
 Wagner, R., & Ellis, W. 1964, *Appl. Phys. Lett.*, 4, 89
 Walker, A., Bohlander, D., & Krelowski, J. 2000, *ApJ*, 530, 362
 Wang, F., Dukovic, G., Brus, L. E., & Heinz, T. F. 2005, *Science*, 308, 838
 Webster, A. 2004, *MNRAS*, 349, 263
 Willacy, K. 2004, *ApJ*, 600, L87
 Zhou, Z., Steigerwald, M., Hybertsen, M., Brus, L., & Friesner, R. 2004, *J. Am. Chem. Soc.*, 126, 3597